Blood–brain barrier permeability in Parkinson's disease patients with and without dyskinesia

Koji Fujita[1], **Shichun Peng**[1], **Yilong Ma**[1], **Chris C. Tang**[1], **Matthew Hellman**[1], **Andrew Feigin**[1], **David Eidelberg**[1], **Vijay Dhawan**[1]

[1]Center for Neurosciences, The Feinstein Institutes for Medical Research, 350 Community Drive, Manhasset, NY 11030, USA

Abstract

Objective—Recent studies on a rodent model of Parkinson's disease (PD) have raised the possibility of increased blood–brain barrier (BBB) permeability, demonstrated by histology, autoradiography, and positron emission tomography (PET). However, in human PD patients, in vivo evidence of increased BBB permeability is lacking. We examined the hypothesis that levodopa treatment increases BBB permeability in human subjects with PD, particularly in those with levodopa-induced dyskinesia (LID).

Methods—We used rubidium-82 (^{82}Rb) and PET to quantify BBB influx in vivo in 19 PD patients, including eight with LID, and 12 age- and sex-matched healthy subjects. All subjects underwent baseline ^{82}Rb scans. Seventeen chronically levodopa-treated patients were additionally rescanned during intravenous levodopa infusion. Influx rate constant, K_1, by compartmental modeling or net influx transport, K_i, by graphical approach could not be estimated reliably. However, V_d, the "apparent volume of distribution" based on the ^{82}Rb concentration in brain tissue and blood, was estimated with good stability as a local measure of the volume of distribution.

Results—Rubidium influx into brain tissue was undetectable in PD patients with or without LID, scanned on and off drug. No significant differences in regional V_d were observed for PD patients with or without LID relative to healthy subjects, except in left thalamus. Moreover, changes in V_d measured off- and on-levodopa infusion were also not significant for dyskinetic and non-dyskinetic subjects.

Conclusion—^{82}Rb PET did not reveal significant changes in BBB permeability in PD patients.

Introduction

Parkinson's disease (PD) is characterized by loss of dopaminergic neurons and is effectively treated by the dopamine precursor, levodopa. Chronic levodopa treatment, however, leads to involuntary rhythmic motions called levodopa-induced dyskinesia (LID) in 30–80% of patients.

Several experimental studies were performed to examine the role of the blood–brain barrier (BBB) in the pathogenesis of LID. In a Gd-DTPA MRI study in the 1-methyl-4-phenyl-1,2,3,6-tetrahyropyridine (MPTP) primate model, no evidence was found for increased BBB permeability in LID animals [1]. The images, however, were acquired in the un-medicated state, using a relatively high-molecular-weight contrast agent. Subsequent work in the 6-hydroxydopamine (6-OHDA) rat dyskinesia model revealed levodopa-related increases in striatal BBB permeability using autoradio-graphic techniques [2] as well as microPET [3]. In line with observations in the rodent model, human postmortem tissue study also disclosed evidence of potential BBB leakage in advanced PD patients with dyskinesia [4].

While these data are consistent with alterations in BBB permeability in human PD, objective evidence to this effect is currently lacking. To determine whether permeability is locally increased by levodopa administration, we used PET with the potassium (K^+) analogue rubidium-82 (^{82}Rb), half-life 76 s, which is sensitive to the disruption of BBB tight junctions. We hypothesized that levodopa causes an increase in striatal BBB permeability, which in addition to the normal large neutral amino acid (LNAA) transport process, results in net influx of the drug into the extravascular space. We also hypothesized that this change is greater in patients with LID compared to their non-LID (NLID) counterparts.

Methods

Subjects

We studied 19 PD patients and 12 healthy control subjects as described elsewhere [5]. The PD patients were divided into two groups based on the presence of LID during an intravenous levodopa infusion (see below). The LID group comprised eight subjects in whom levodopa infusion caused sustained dyskinesia. Study details for these subjects are provided in Table 1. The non-LID (NLID) group comprised 11 subjects: nine had stable motor responses to levodopa infusion without; two were drug-naïve. The clinical characteristics of the two PD groups are provided in Table 2. The study was approved by the Institutional Review Board of Northwell Health. Written informed consent was obtained from all participants.

Positron emission tomography

The PD patients and the control subjects underwent baseline ^{82}Rb PET (saline infusion) after fasting overnight and/or consuming a very low-protein breakfast at least 4 h prior to the PET study. Oral dose of 200 mg carbidopa was administered one hour prior to the levodopa infusion. In the chronically treated PD patients, antiparkinsonian medications were withheld at least 12 h before imaging. UPDRS motor ratings were obtained prior to imaging in all PD patients. Those on daily oral medication ($n = 17$) were rescanned on the same day during an intravenous levodopa infusion as detailed elsewhere [5, 6]. In each PD subject, drug infusion was titrated to achieve 20–40% improvement in UPDRS motor ratings for at least 30 min before the start of imaging, with < 10% change in UPDRS ratings obtained at subsequent 30-min intervals. In the LID subjects, the rate of levodopa infusion was determined by the initiation of dyskinesia, which was usually within 30 min. The levodopa infusion rate was then adjusted to reduce the induced, involuntary movements to a minimum (average infusion rate: 1.2 ± 0.6 mg/kg/h). PD and healthy control subjects were additionally scanned with [^{15}O]-water (H$_2^{15}$O) and [^{18}F]-fluorodeoxyglucose (^{18}FDG) PET before and during the infusion as part of a larger protocol as described elsewhere [5, 7]. A flowchart of the radiotracer studies that were conducted is provided in Fig. 1.

A 10-min transmission scan was performed before the PET scan. 740 MBq (20 mCi) of ^{82}Rb, eluted from a ^{82}Sr/^{82}Rb generator (Bracco Diagnostics Inc., Monroe Township, NJ) in normal saline was injected as an intravenous bolus for approximately 20 s. Serial PET images were acquired for 6 min (1×20 s, 1×10 s, 6×5 s, 4×7 s, 7×30 s, and 1×62 s; Fig. 2) in three-dimensional mode using the GE Advance PET scanner (GE Medical Systems, Milwaukee, WI). This eight-ring bismuth-germanate scanner provided 35 two-dimensional image planes with transaxial resolution of 4.2 mm in all directions. All PET studies were performed in the rest state with the subjects' eyes open in a dimly lit room with minimal auditory stimulation.

Data analysis

Preprocessing of all image data was performed using Statistical Parametric Mapping (SPM) 5 (http://www.fil.ion.ucl.ac.uk/spm/) run on MATLAB 7.3.0. Dynamic ^{82}Rb PET images were realigned for motion corrections across time series and then spatially normalized using the same spatial transformation parameters determined between individual transmission PET image and transmission PET image template in a standard brain space. The PET images were smoothed with an isotropic Gaussian kernel full-width at half maximum of 10 mm. The concentration in tissue (C_t) was measured in anatomical regions-of-interest (ROIs), as well as predefined volumes-of-interest (VOIs) based on a priori information using Scan Analysis and Visualization Processor software (http://feinsteinneuroscience.org). We evaluated C_t in the bilateral anterior cingulate cortex, posterior putamen, and thalamus as aromatic L-amino acid decarboxylase-rich (AADC) regions, as well as in the right superior temporal gyrus and inferior parietal lobule (which have low AADC expression) as control regions. The pre-determined VOIs were 3-mm-radius spheres centered at four coordinates in the putamen and thalamus, in which significant levodopa-mediated dissociation of cerebral blood flow and glucose metabolism was discerned in the same PD patient sample [5]. The concentration in blood (C_b) was measured in a 3-mm-radius sphere centered in the

superior sagittal sinus. Additionally, we calculated the volume of distribution (V_d) for each of the regions as the average of C_t/C_b of the last 7 frames spanning 2–6 min (see Appendix. Modeling approach, power calculations), which was compared between groups and conditions.

Comparison between normal controls and patients with and without LID was performed using ANOVA with post hoc Tukey–Kramer HSD correction for multiple comparisons. The difference between values measured on and off levodopa was assessed separately for PD patients in the LID and NLID groups using paired t tests. Statistical analyses were conducted using SPSS version 22 (IBM Corporation, Armonk, NY). Results were considered significant at $p < 0.05$.

Results

Given that K_1 and K_i could not be estimated in the ^{82}Rb PET data (see discussion of the modeling approach in the Appendix), we concluded that substantial alterations in BBB were not present on- or off-levodopa infusion. We did, however, use the data to estimate V_d as a measure of the changes in distribution volume in AADC-rich regions in the posterior putamen, thalamus, and anterior cingulate cortex (see Methods). V_d measurements were then used to determine whether distribution volume is altered in one or more of these regions, particularly in areas found previously to exhibit significant levodopa-mediated flow-metabolism dissociation in the same population [5]. We found no significant difference in baseline V_d measured in these regions (Fig. 3) in the PD group as a whole, or in the LID and NLID subgroups compared to healthy control subjects ($p > 0.1$). A sole exception is the left thalamus in which a significant increase in the off-state was observed in LID compared to NLID ($F[2,28] = 3.85$, $p = 0.033$; Tukey–Kramer HSD). Likewise, no significant V_d changes were seen (Fig. 3) for within-subject differences between baseline and on-state values in these brain regions (see Fig. 4).

Discussion

Abnormal increases in local BBB permeability were not seen with ^{82}Rb PET in LID or NLID PD patients, whether scanned in the un-medicated baseline state or during levodopa infusion. The current results contrast with the striking changes seen under comparable pharmacological conditions in the 6-OHDA rodent dyskinesia model [2, 3]. We note that the rodent dyskinetic model differs from human LID in a number of respects. First, while the experimental model is based upon acute and local injury of the ascending dopamine fiber bundle by 6-OHDA injection, human PD develops insidiously with widespread pathology that is not limited to the nigrostriatal pathway. More important perhaps is the dosage of levodopa which was substantially larger in rodent compared to the human [3]. Lastly, the method used to assess BBB permeability in the experimental model is different than that used in the human PD study. In the rodent model, α-aminoisobutyric acid (AIB), a neutral amino acid, was used. This tracer can cross intact endothelial cells as well as disrupted tight junctions of the BBB. It is primarily transported across BBB endothelial cells by the amino acid transporter A system, and also by the L and ASC systems [8]. By contrast, ^{82}Rb does not depend on amino acid transport and therefore is not likely to be influenced

by levodopa in the same way. That being said, substantial evidence exists apart from AIB uptake measurements in the rodent to implicate dysfunction of the striatal neurovascular unit in the pathogenesis of LID in human PD [4, 9, 10].

Our study was based upon animal data suggesting tight junction opening as a cause for BBB permeability. Therefore, ^{82}Rb, a potassium analog that crosses the BBB independently of the LNAA transporter system, was selected to detect changes at tight junctions induced by levodopa. That said, pharmacological modulation of LNAA transporters may be another cause for permeability changes as seen with radiolabeled AIB in rodent studies. The LNAA transport system has been extensively studied, and up- and-down regulation has been reported. In particular, (1) plasma amino acid levels compete with and can decrease levodopa uptake in the brain [11, 12]; (2) endotoxin-induced inflammation can down-regulate L-type amino acid BBB transporter 1 (LAT1) in rodents [13]; (3) Up-regulation of LAT1 is well established in oncology and has been successfully used in imaging tumors [14]. However, up-regulation of LAT1 for the chronic levodopa treatment has not been reported in PD.

Other radiotracers can be used to assess LAT1 transporter function, such as [^{18}F]-3-*O*-methyl-dopa (3-OMFD) and [^{11}C]-methylaminoisobutyric acid (MeAIB). In an [^{18}F]-3-OMFD PET study in human PD, we found that the kinetics of this tracer were similar to that of [^{18}F]-FDOPA, but with small regional differences [15]. Studies using 3-OMFD can be performed in the early disease stage (off-levodopa), but data analysis is complicated in the on-levodopa dyskinesia state by interactions between levodopa metabolites and the radiotracer. [^{11}C]-MeAIB, as with [^{11}C]-AIB, would be subject to LNAA transporter modulations (especially the A, ASC, and L systems) in the course of levodopa administration.

Future off-state studies can be undertaken with either of these tracers, although long-duration dynamic scans, particularly in LID patients, may be difficult to perform. Methods to differentiate changes in tight junctions from LNAA transporters will be helpful, such as a recently developed non-contrast MRI technique [16].

Estimation of the influx constant K_1 as a direct measure of BBB permeability was not possible in the PD or the healthy control subjects. Nonetheless, using V_d as a measure of distribution volume changes and possibly an indirect reflection of angiogenesis, we found no evidence of change in the apparent volume of distribution in PD patients with LID, relative to control subjects or subjects without LID except for the left thalamus in the "off" state. The enhanced cerebral blood flow response to levodopa in the left thalamus observed in LID subjects [17] may therefore reflect a change in V_d, at least in part.

Even though a number of radiotracers for angiogenesis have been developed for oncologic use, none to date are suitable to detect the localized, low magnitude changes observed in experimental LID. Vasodilation resulting from levodopa infusion [18] can be confirmed using C^{15}O PET, but these studies were not performed because of concerns over radiation dose. The issues attendant to absolute values of K_1 and V_d for ^{82}Rb PET are further discussed in the Appendix.

Finally, we speculate that for very low K_1 values the [82]Rb bolus technique may not be able to estimate very small changes in influx accurately because of the short half-life of the tracer and the correspondingly short scan duration. This issue may be addressed using a constant infusion technique. That, however, would require a separate blood volume study and additional radiation exposure. The possibility of a small, highly localized levodopa-mediated permeability change in PD generally, and in LID in particular, cannot be excluded based on the current data.

A number of technical issues attendant to [82]Rb PET are also worthy of mention. We did not sample the tracer in the blood during scanning because of the complexity of the necessary protocol. For a primarily intravascular radiotracer, such as [82]Rb, a curve derived from radioactivity measurements in one of the large cerebral blood vessels is theoretically a better representation of the arterial input function than actually sampling radial arterial blood (with associated smearing). Deriving input function from images also makes the procedure more tolerable to the subjects. In human [18]FDG PET studies, a close relationship between carotid artery image-derived function (IDF) and actual arterial sampled curves has been demonstrated [19]. However, the absolute scale of the IDF cannot be accurately determined without actual sampling of peripheral blood for calibration, which was not done here. Lastly, to reduce motion artifacts, we titrated the levodopa infusion to just below the dyskinesia threshold. Thus, the possibility exists that a significant increase was not observed in the absence of LID. Indeed, given the limited number of subjects in the current study and the complex nature of the imaging protocol, the results may not be generalizable to the PD population at large.

Conclusion

Our findings do not support the presence of significant alterations in BBB permeability in PD patients with or without LID. The possibility of small, highly localized permeability changes in PD cannot be completely excluded using our [82]Rb PET method. Increased off-state V_d in the left thalamus of LID subjects in the off-state is an interesting finding, which will require further confirmation.

Acknowledgments

Funding

Availability of data and material

The datasets generated during and/or analyzed during the current study are available from the corresponding author on reasonable request.

Appendix

Modeling approach

Direct and the preferred parameter for BBB permeability is influx constant, K_1 or net unidirectional rate constant, Ki. We attempted a full compartmental modeling including K_1 (influx from blood to brain), k_2 (efflux from brain to blood), and V_b (cerebral tissue blood volume), as in our previous work [20–22]. However, estimated parameters of K_1 and k_2 were very unstable with unacceptably large errors and frequent failure of the regression routine to converge. Reasonable curve-fits were obtained only with volume parameter. We also tried other models with k_2 assumed as 0 and multiple-time graphical approach for estimating K_i [23], without much success. Then we inspected the tissue and blood curves (C_t and C_b) more carefully and noticed that the shapes of both curves were similar and appeared to be parallel after 2 min. We calculated the ratio of C_t and C_b, and discovered that this ratio was essentially constant from 2 to 6 min of scan duration. This ratio was defined as apparent volume of distribution (V_d). Next, we scaled the tissue curve using this ratio and found that the scaled tissue curve superimposed the blood curve, suggesting that there was negligible uptake process, i.e., transfer of ^{82}Rb across the BBB, and that the tissue curve was just a scaled version of the blood curve (for significant uptake of tracer into the extravascular compartment, the brain time–activity curve shifts to the right of the blood curve and exceeds the level of blood curve at later times [20]). We confirmed this in each case using the Kolmogorov–Smirnov test (Appendix Table 3). We also compared carotid artery-derived time–activity curves with those derived from the sagittal sinus. They were similar except the carotid curves had marginally more noise in the later phase of the study. All these findings were observed in PD cohorts as well as in healthy control subjects.

Power calculations

Because MRI studies of BBB in Alzheimer's disease have suggested an at least two-fold increase in KTrans [24], we assumed that a minimal mean K_1 value of 0.008 is expected for increased BBB permeability in PD which corresponds to a two-fold increase over the mean K_1 value of 0.004 ($\pm$ 0.003, SD) for control brain regions [20]. With this effect size (1.33), our study with the same sample size of 19 PD and 12 normal control subjects would achieve a power of 0.94 at $a = 0.05$ to detect this level of change in K_1 (two-sample Student's t-test, two-sided). If the calculation was limited to the 8 LID patients and the 12 normal control subjects, a power of 0.79 would be achieved at $a = 0.05$. Our study would therefore be slightly underpowered to detect a significant change in this parameter.

K_1 and V_d absolute values

Small but non-zero K_1 values were obtained from our studies in the 1980's (0.007 ml/min/g). The explanation for our study is that in those studies [20] all subjects had

glioblastomas with likely damage to the BBB. Even the control region (mislabeled "normal tissue" in some of our publications) should have been correctly labeled only as "contralateral tissue" that was subjected to acute radiation exposure of 400–1800 rad or centigray and thus, in reality, not a true normal tissue anymore. It is a well-known fact that whole brain radiation treatment causes BBB permeability increases. We also speculate that a short study duration of 6 min may not be enough to accurately separate brain and blood activity curves in situations of very low permeability (due to not enough buildup of radioactivity in the brain tissue and a large positron range of Rb82).

Our values for Vd are almost 10 times larger than cerebral blood volume. The reason could be (1) that the sagittal sinus activity is 10 times lower than actual arterial activity probably due to lack of partial volume correction (PVC), which is unlikely given the number of previous publications demonstrating similarity of these two methods to estimate input functions. A smaller scaling factor is, however, possible in the absence of blood sampling; and (2) more likely, the high Vd values may be explained by the artificially higher brain tissue curve due to spillover effect which would have caused an increase in the value of tissue curve yielding higher Vd values without affecting the group comparisons of Vd values in the OFF and ON conditions.

The absolute value of IDF is expected to have a scaling effect which can change the absolute value of V_d but have essentially a very small effect upon the influx constant K_1 due to marginal change in the shape of the curve. The increase in absolute value of IDF by implementing partial volume correction will cause further reduction in the value of K_1. Changes in V_d, if any, will have similar effects for both ON and OFF levodopa infusion. Combined Partial volume and/or spillover effect corrections may lower Vd values to a more physiological range at the cost of additional noise.

References

1. Astradsson A, Jenkins BG, Choi J-K, Hallett PJ, Levesque MA, McDowell JS, Brownell A-L, Spealman RD, Isacson O (2009) The blood–brain barrier is intact after levodopa-induced dyskinesias in parkinsonian primates—evidence from in vivo neuroimaging studies. Neurobiol Dis 35:348–351 [PubMed: 19501164]

2. Ohlin KE, Sebastianutto I, Adkins CE, Lundblad C, Lockman PR, Cenci MA (2012) Impact of L-DOPA treatment on regional cerebral blood flow and metabolism in the basal ganglia in a rat model of Parkinson's disease. Neuroimage 61:228–239 [PubMed: 22406356]

3. Lerner RP, Francardo V, Fujita K, Bimpisidis Z, Jourdain VA, Tang CC, Dewey SL, Chaly T, Cenci MA (2017) Levodopa-induced abnormal involuntary movements correlate with altered permeability of the blood-brain-barrier in the basal ganglia. Sci Rep 7:16005. 10.1038/s41598-017-16228-1 [PubMed: 29167476]

4. Ohlin KE, Francardo V, Lindgren HS, Sillivan SE, O'Sullivan SS, Luksik AS, Vassoler FM, Lees AJ, Konradi C, Cenci MA (2011) Vascular endothelial growth factor is upregulated by l-dopa in the parkinsonian brain: implications for the development of dyskinesia. Brain 134:2339–2357 [PubMed: 21771855]

5. Jourdain VA, Tang CC, Holtbernd F, Dresel C, Choi YY, Ma Y, Dhawan V, Eidelberg D (2016) Flow-metabolism dissociation in the pathogenesis of levodopa-induced dyskinesia. JCI Insight 1(15):e86615. 10.1172/jci.insight.86615 [PubMed: 27699242]

6. Hirano S, Asanuma K, Ma Y, Tang C, Feigin A, Dhawan V, Carbon M, Eidelberg D (2008) Dissociation of metabolic and neurovascular responses to levodopa in the treatment of Parkinson's disease. J Neurosci 28:4201–4209 [PubMed: 18417699]

7. Jourdain VA, Schindlbeck KA, Tang CC, Niethammer M, Choi YY, Markowitz D, Nazem A, Nardi D, Carras N, Feigin A, Ma Y, Peng S, Dhawan V, Eidelberg D (2017) Increased putamen hypercapnic vasoreactivity in levodopa-induced dyskinesia. JCI Insight 2(20):e96411. 10.1172/jci.insight.96411 [PubMed: 29046477]

8. Bass R, Hedegaard HB, Dillehay L, Moffett J, Englesberg E (1981) The A, ASC, and L systems for the transport of amino acids in Chinese hamster ovary cells (CHO-K1). J Biol Chem 256:10259–10266 [PubMed: 7287709]

9. Janelidze S, Lindqvist D, Francardo V, Hall S, Zetterberg H, Blennow K, Adler CH, Beach TG, Serrano GE, van Westen D, Londos E, Cenci MA, Hansson O (2015) Increased CSF biomarkers of angiogenesis in Parkinson disease. Neurology 85:1834–1842 [PubMed: 26511451]

10. Gray MT, Woulfe JM (2015) Striatal blood-brain barrier permeability in Parkinson'S disease. J Cereb Blood Flow Metab 35:747–750 [PubMed: 25757748]

11. Puris E, Gynther M, Auriola S, Huttunen KM (2020) L-Type amino acid transporter 1 as a target for drug delivery. Pharm Res 37:88 [PubMed: 32377929]

12. Alexander GM, Schwartzman RJ, Grothusen JR, Gordon SW (1994) Effect of plasma levels of large neutral amino acids and degree of parkinsonism on the blood-to-brain transport of levodopa in naive and MPTP parkinsonian monkeys. Neurology 44:1491–1499 [PubMed: 8058155]

13. Wittmann G, Mohácsik P, Balkhi MY, Gereben B, Lechan RM (2015) Endotoxin-induced inflammation down-regulates l-type amino acid transporter 1 (LAT1) expression at the blood–brain barrier of male rats and mice. Fluids Barriers CNS 12:21 [PubMed: 26337286]

14. Nishii R, Higashi T, Kagawa S, Arimoto M, Kishibe Y, Takahashi M, Yamada S, Saiki M, Arakawa Y, Yamauchi H, Okuyama C, Hojo M, Munemitsu T, Sawada M, Kobayashi M, Kawai K, Nagamachi S, Hirai T, Miyamoto S (2018) Differential diagnosis between low-grade and high-grade astrocytoma using system a amino acid transport PET imaging with C-11-MeAIB: a comparison study with C-11-methionine PET imaging. Contrast Media Mol Imaging 2018:9. 10.1155/2018/1292746

15. Dhawan V, Ishikawa T, Patlak C, Chaly T, Robeson W, Belakhlef A, Margouleff C, Mandel F, Eidelberg D (1996) Combined FDOPA and 3OMFD PET studies in Parkinson's disease. J Nucl Med 37:209–216 [PubMed: 8667046]

16. Lin Z, Li Y, Su P, Mao D, Wei Z, Pillai JJ, Moghekar A, van Osch M, Ge Y, Lu H (2018) Non-contrast MR imaging of blood-brain barrier permeability to water. Magn Reson Med 80:1507–1520 [PubMed: 29498097]

17. Hershey T, Black KJ, Stambuk MK, Carl JL, Mcgee-Minnich LA, Perlmutter JS (1998) Altered thalamic response to levodopa in Parkinson's patients with dopa-induced dyskinesias. Proc Natl Acad Sci USA 95:12016–12021 [PubMed: 9751782]

18. Krimer LS, Muly EC, Williams GV, Goldman-Rakic PS (1998) Dopaminergic regulation of cerebral cortical microcirculation. Nat Neurosci 1:286–289 [PubMed: 10195161]

19. Chen K, Chen X, Renaut R, Alexander GE, Bandy D, Guo H, Reiman EM (2007) Characterization of the image-derived carotid artery input function using independent component analysis for the quantitation of [18F] fluorodeoxyglucose positron emission tomography images. Phys Med Biol 52:7055–7071 [PubMed: 18029993]

20. Jarden JO, Dhawan V, Poltorak A, Posner JB, Rottenberg DA (1985) Positron emission tomographic measurement of blood-to-brain and blood-to-tumor transport of 82Rb: The effect of dexamethasone and whole-brain radiation therapy. Ann Neurol 18:636–646 [PubMed: 3878686]

21. Dhawan V, Poltorak A, Moeller JR, Jarden JO, Strother SC, Thaler H, Rottenberg DA (1989) Positron emission tomographic measurement of blood-to-brain and blood-to-tumour transport of 82 Rb. I: Error analysis and computer simulations. Phys Med Biol 34:1773–1784 [PubMed: 2616637]

22. Dhawan V, Jarden JO, Moeller JR, Strother SC, Rottenberg DA (1989) Positron emission tomographic measurement of blood-to-brain and blood-to-tumour transport of 82 Rb. II: clinical data and validation of technique. Phys Med Biol 34:1785–1794 [PubMed: 2616638]

23. Patlak CS, Blasberg RG, Fenstermacher JD (1983) Graphical evaluation of blood-to-brain transfer constants from multiple-time uptake data. J Cereb Blood Flow Metab 3:1–7 [PubMed: 6822610]

24. van de Haar HJ, Burgmans S, Jansen JFA, van Osch MJP, van Buchem MA, Muller M, Hofman PAM, Verhey FRJ, Backes WH (2016) Blood-brain barrier leakage in patients with early Alzheimer disease. Radiology 281:527–535 [PubMed: 27243267]

Day 1

UPDRS

200mg Carbidopa

50mg Carbidopa

Levodopa Infusion

Time approx. (min)

| 0 | 60 | 70 | 80 | 90 100 | 160 | 170 | 180 | 190 |

$H_2^{15}O$ $H_2^{15}O$ ^{82}Rb ^{82}Rb $H_2^{15}O$ $H_2^{15}O$ ^{82}Rb ^{82}Rb

Day 2

$H_2^{15}O$ Quality control

Start 5% CO_2 Inhalation

End 5% CO_2 Inhalation

Time approx. (min)

| 0 | 10 | 20 | 30 | 31.5 | 33 | 40 | 90 |

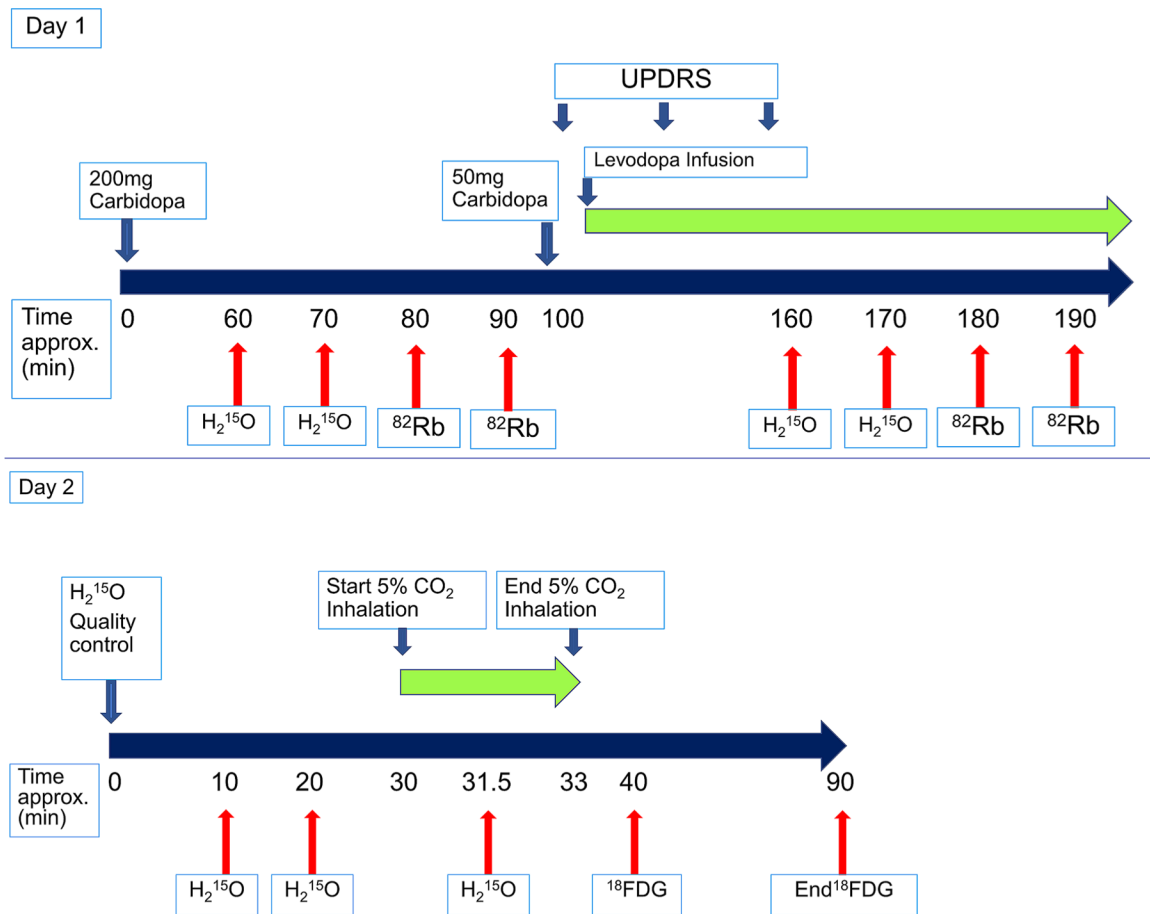$H_2^{15}O$ $H_2^{15}O$ $H_2^{15}O$ ^{18}FDG End ^{18}FDG

Fig. 1.

Flowchart for the PET studies. Day1. **a** [^{15}O]-water ($H_2^{15}O$) PET studies for cerebral blood flow and ^{82}Rb bolus injection for BBB permeability performed in the baseline off-state and during levodopa infusion. Day2. **b** $H_2^{15}O$ PET bolus studies in the off-state during normocapnia (room air) and during hypercapnia (5% CO_2 rebreathing) [7]. [^{18}F]-FDG PET for cerebral glucose metabolism before and during levodopa infusion was conducted as described previously [5]
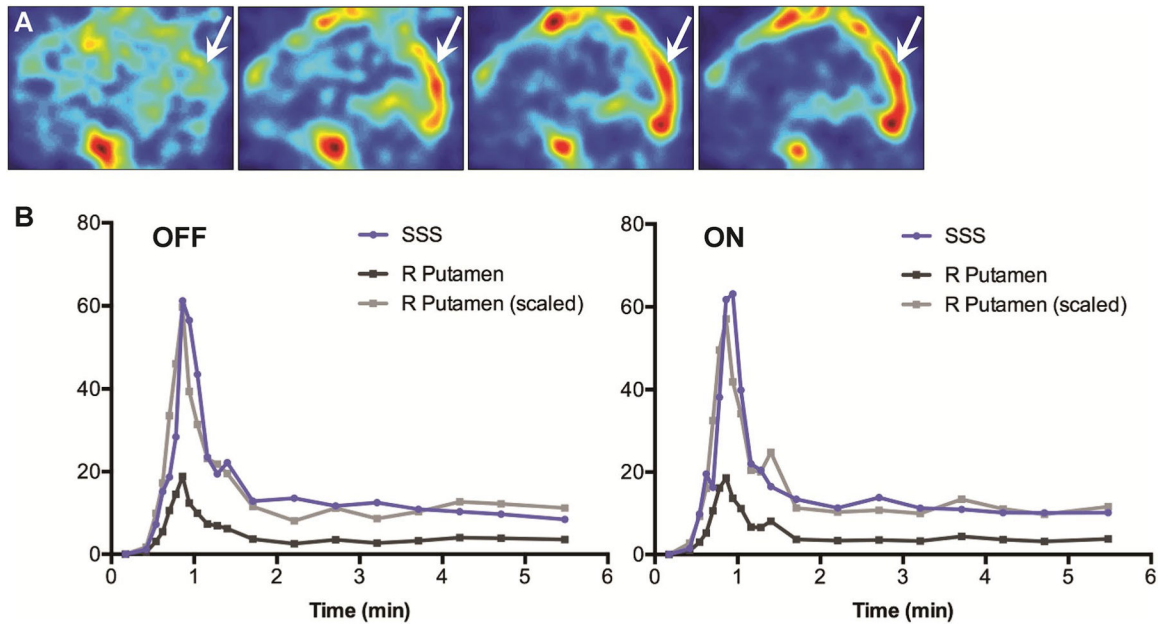
Fig. 2.

Rubidium-82 time–activity curves in sagittal sinus and putamen. **a** We obtained serial rubidium-82 scans for 6 min after bolus injection for each subject and condition. The images shown correspond to those at 43, 48, 53, and 58 s in a subject. The radioactivity in the superior sagittal sinus (SSS, arrows) reached a peak at approximately 1 min. **b** Time activity curves show rubidium-82 activity during OFF (saline infusion) and ON (levodopa infusion) in a subject. The time course was similar in the right putamen (black) and the SSS (blue). The scaled activity in the putamen (gray) largely overlapped with the SSS activity (blue), suggesting that there was no transfer of rubidium-82 across the blood–brain barrier
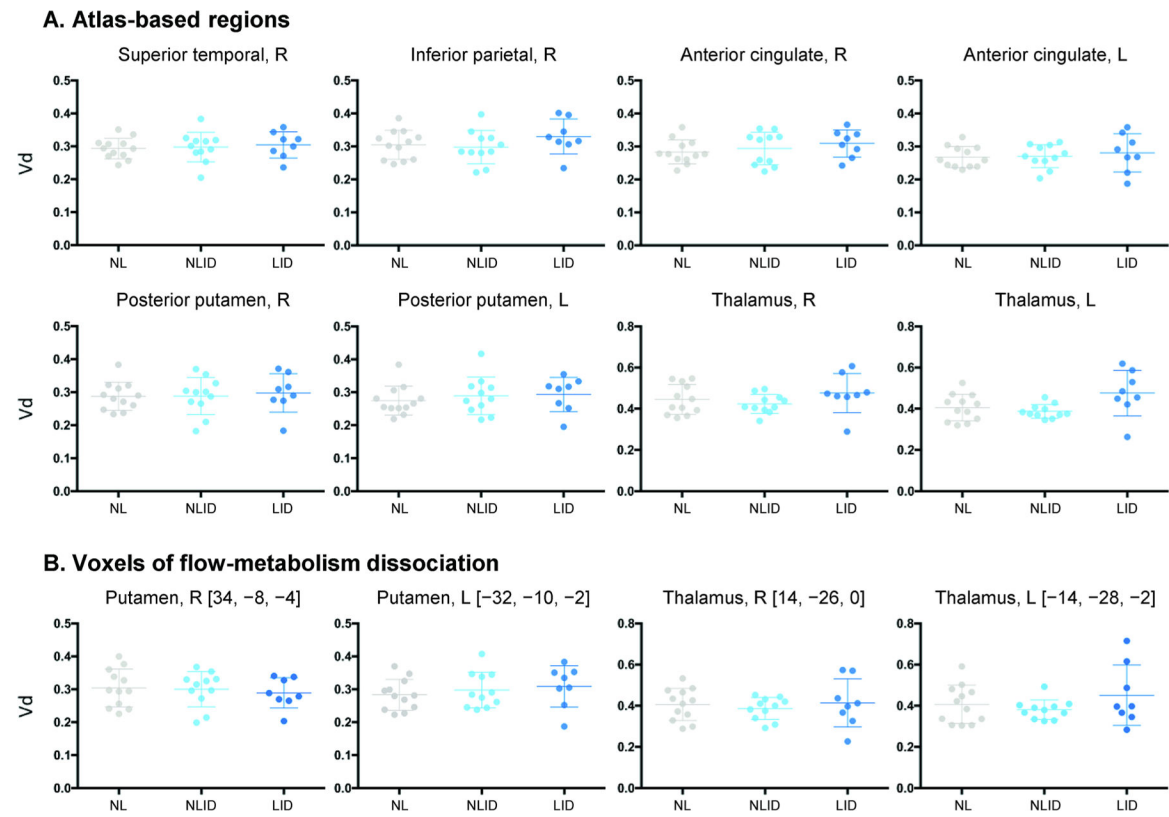
Fig. 3.

Volume of distribution in various regions in normal, LID, and NLID. We compared apparent volume of distribution (V_d), which served as a measure of tissue vascular space, between the normal controls (NL) and patients with Parkinson's disease in the OFF state (saline infusion). The patients were classified into two groups according to the absence or presence of levodopa-induced dyskinesia (LID). **a** We measured V_d in the atlas-based regions-of-interest that included aromatic L-amino acid decarboxylase-rich regions, and found no significant increases except in the left thalamus of LID subjects (one-way ANOVA, $p = 0.032$ with post-hoc correction for multiple comparisons using Tukey–Kramer HSD). **b** We also measured V_d in the volumes-of-interest in which we previously reported flow-metabolism dissociation, and found no significant differences. *NLID* non-LID

A. Atlas-based regions
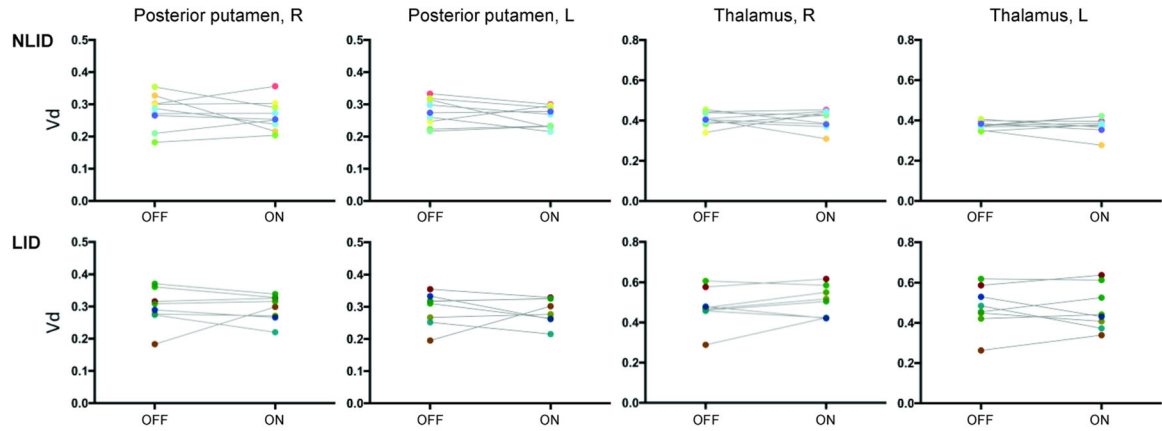
B. Voxels of flow-metabolism dissociation
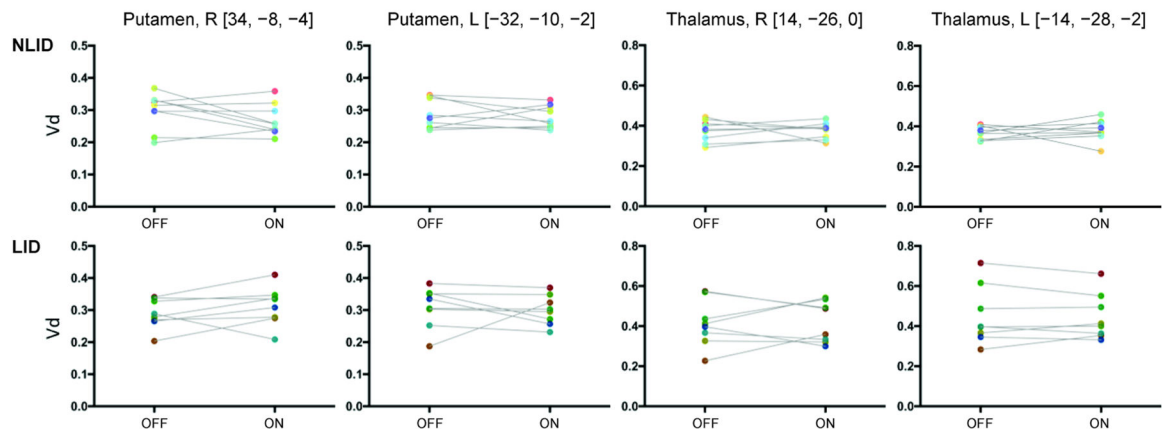
Fig. 4.
Volume of distribution during saline and levodopa infusion in aromatic ʟ-amino acid decarboxylase-rich regions. We compared volume of distribution (V_d) between saline infusion (OFF) and levodopa infusion (ON) conditions in Parkinson's disease patients with or without levodopa-induced dyskinesia (LID). We detected no significant V_d changes in the aromatic ʟ-amino acid decarboxylase (AADC)-rich regions-of-interest as well as ROIs devoid of AADC (**a**) or the volumes-of-interest of flow-metabolism dissociation (**b**). *NLID* non-LID

Table 1

Study details for individual LID subjects

Subject	Age (years)	Sex	Weight (Kg)	Disease duration	H&Y	LEDD (mg/Kg/day)	LEDD (mg/Kg/day)	LD infused (mg/Kg/h)	UPDRS OFF	UPDRS ON	UPDRS change(%)	UPDRS-IV
1	56	M	69.85	5	2	400	5.717	0.429	25	13	48.0	1
2	53	F	52.16	9	2	550	10.527	0.957	18	8	55.6	3
3	59	M	78.93	9	2	600	7.590	0.632	23	7	69.6	1
4	55	M	99.79	12	2	950	9.504	2.001	29	14	51.7	1
5	56	M	56.70	16	2	700	12.326	0.880	29	13	55.2	2
6	60	M	76.36	7	2	660	8.647	1.041	26	13	50.0	2
7	67	F	62.73	13	3	850	13.557	1.216	27	22	18.5	2
8	67	F	81.82	6	2	898	10.981	2.202	22	10	54.5	1
Mean	59.1		72.3	9.6	2.1	701.0	9.9	1.2	24.9	12.5	50.4	1.6
SD	5.3		15.4	3.8	0.4	188.3	2.5	0.6	3.8	4.6	14.4	0.7

H&Y Hoehn and Yahr scale, *LDD* levodopa daily dose, *LDD(w)* weight-corrected levodopa daily dose, *LEDD* levodopa equivalent daily dose, *LEDD(w)* weight-corrected levodopa equivalent daily dose, *LID* Parkinson's disease subjects with levodopa-induced dyskinesia, *non-LID* Parkinson's disease subjects without LID, *UPDRS* Unified Parkinson's Disease Rating Scale, *UPDRS-IV* dyskinesia severity

Table 2

Clinical profiles of patients with Parkinson's disease

	Non-LID (*n* = 11)	LID (*n* = 8)	
Age (years)	68.0 ± 8.5^a	59.1 ± 5.3	*
Sex (M:F)	8:3	5:3	n.s
Disease duration (years)	6.5 ± 4.8	9.6 ± 3.8	n.s
Hoehn and Yahr stage (OFF)	1.8 ± 0.6	2.1 ± 0.4	n.s
UPDRS part III (OFF)	19.4 ± 5.9	24.9 ± 3.8	*
UPDRS part III (ON)	12.3 ± 5.2	17.0 ± 6.2	n.s
UPDRS part III change (%)	38.1 ± 20.9	50.4 ± 14.4	n.s
LDD (mg/day)	361.1 ± 179.9	805.6 ± 300.1	**
LDD(w) (mg/kg/day)	4.7 ± 1.8	11.5 ± 4.9	**
LEDD (mg/day)	510.9 ± 253.0	701.0 ± 188.3	*
LEDD(w) (mg/kg/day)	6.6 ± 2.9	9.9 ± 2.5	**

H&Y Hoehn and Yahr scale, *LDD* levodopa daily dose, *LDD(w)* weight-corrected levodopa daily dose, *LEDD* levodopa equivalent daily dose, *LEDD(w)* weight-corrected levodopa equivalent daily dose, *LID* Parkinson's disease subjects with levodopa-induced dyskinesia, *non-LID* Parkinson's disease subjects without LID, *UPDRS* Unified Parkinson's Disease Rating Scale, *UPDRS-IV* dyskinesia severity

*
$p < 0.05$,

**
$p < 0.01$;

Student's *t* tests for comparison of non-LID vs. LID

*A*Data presented as mean ± SD

Table 3

Comparisons of time–activity curves between tissue and blood

Healthy subjects			Parkinson's disease patients					
Subject no	OFF	ON	Subject no	Non-LID		Subject no	LID	
				OFF	ON		OFF	ON
1	$p = 0.954$	–	**13**	$p = 0.56$	–	**24**	$p = 0.819$	$p = 0.978$
2	$p = 0.983$	–	**14**	$p = 0.978$	–	**25**	$p = 0.172$	$p = 0.978$
3	$p = 0.978$	–	**15**	$p = 0.978$	$p = 0.819$	**26**	$p = 0.978$	$p = 0.978$
4	$p = 0.978$	–	**16**	$p = 0.978$	$p = 0.329$	**27**	$p = 0.978$	$p = 0.978$
5	$p = 0.259$	–	**17**	$p = 0.329$	$p = 0.978$	**28**	$p = 0.819$	$p = 0.819$
6	$p = 0.59$	–	**18**	$p = 0.978$	$p = 0.978$	**29**	$p = 0.978$	$p = 0.978$
7	$p = 0.983$	–	**19**	$p = 0.978$	$p = 0.819$	**30**	$p = 0.819$	$p = 0.819$
8	$p = 0.978$	–	**20**	$p = 0.978$	$p = 0.978$	**31**	$p = 0.56$	$p = 0.819$
9	$p = 1$	–	**21**	$p = 0.56$	$p = 0.56$			
10	$p = 1$	–	**22**	$p = 0.819$	$p = 0.978$			
11	$p = 0.819$	–	**23**	$p = 0.978$	$p = 0.56$			
12	$p = 0.819$	–						

We found no significant difference in time-dependent activity changes between scaled brain tissue (thalamus) and blood (sagittal sinus) (two-sample Kolmogorov–Smirnov test)

LID levodopa-induced dyskinesia, *OFF* during saline infusion, *ON* during levodopa infusion

Bold values indicate that the differentiate PD from normal subjects